


# Characterization of Strain Due to Nitrogen Doping Concentration Variations in Heavy Doped 4H-SiC

YU YANG <sup>1,2</sup> JIANQIU GUO,<sup>1,3</sup> BALAJI RAGHOTHAMACHAR,<sup>1,4</sup>  
XIAOJUN CHAN,<sup>1,5</sup> TAEJIN KIM,<sup>1,6</sup> and MICHAEL DUDLEY<sup>1,7</sup>

1.—Department of Materials Science and Engineering, Stony Brook University, Stony Brook, NY 11794, USA. 2.—e-mail: yu.yang@stonybrook.edu. 3.—e-mail: jianqiu.guo@stonybrook.edu. 4.—e-mail: balaji.raghothamachar@stonybrook.edu. 5.—e-mail: xiaojun.chan@stonybrook.edu. 6.—e-mail: taejin.kim@stonybrook.edu. 7.—e-mail: michael.dudley@stonybrook.edu

Highly doped 4H-SiC will show a significant lattice parameter difference with respect to the undoped material. We have applied the recently developed monochromatic contour mapping technique for 4H-SiC crystals to a 4H-SiC wafer crystal characterized by nitrogen doping concentration variation across the whole sample surface using a synchrotron monochromatic x-ray beam. Strain maps of 0008 and  $-2203$  planes were derived by deconvoluting the lattice parameter variations from the lattice tilt. Analysis reveals markedly different strain values within and out of the basal plane indicating the strain induced by nitrogen doping is anisotropic in the 4H-SiC hexagonal crystal structure. The highest strain calculated along growth direction  $[0001]$  and along  $[1-100]$  on the closed packed basal plane is up to  $-4 \times 10^{-4}$  and  $-2.7 \times 10^{-3}$ , respectively. Using an anisotropic elasticity model by separating the whole bulk crystal into numerous identical rectangular prism units, the measured strain was related to the doping concentration and the calculated highest nitrogen level inside wafer crystal was determined to be  $1.5 \times 10^{20} \text{ cm}^{-3}$ . This is in agreement with observation of double Shockley stacking faults in the highly doped region that are predicted to nucleate at nitrogen levels above  $2 \times 10^{19} \text{ cm}^{-3}$ .

**Key words:** Nitrogen doping concentration, 4H-SiC, heavy doped, contour mapping, anisotropic strain

## INTRODUCTION

4H-SiC is a promising wide bandgap material that has attracted considerable attention in the power electronics industry. Several applications have benefited from the improved performance of devices made of 4H-SiC in terms of higher breakdown fields, efficiency, and reliability, as well as excellent physical properties.<sup>1</sup>

However, the widespread commercialization of this material is still hindered by the various defects introduced during the crystal growth, which is found to degrade the device performance and

lifetime. Stacking faults (SFs), for example, have been considered to be one of the most detrimental structural defects.<sup>2</sup> The extra states introduced by SFs can prevent the normal build-up of an electron-hole plasma, which leads to a forward voltage drop with time during device operation. The electrical degradation caused by stacking faults in 4H-SiC pin diodes has been reported in the literature.<sup>2</sup> It has been predicted theoretically that high nitrogen doping concentration level (above  $2 \times 10^{19} \text{ cm}^{-3}$ ) inside 4H-SiC crystals increases the propensity for formation of stacking faults [ref]. The SFs inside can create quantum wells, which lower the free energy of the whole crystal once the barrier for partial dislocation motion is overcome by thermal energy (achieved by annealing above  $1000^\circ\text{C}$ ).<sup>3,4</sup> Moreover, from a perspective of high power electronic

applications, other severe issues, such as inhomogeneous resistivity and a large {0001} surface roughness of substrate are characteristic of heavily nitrogen-doped SiC crystals.<sup>5</sup> Further, the nitrogen incorporation kinetics is anisotropic within and outside the basal plane during PVT growth of SiC. Therefore, a better understanding of the nitrogen doping distribution within the SiC wafers is important.

Highly doped 4H-SiC can have a significant lattice distortion due to the impurity incorporation process. The 4H-SiC crystal can be considered as an assembly of periodic organized tetrahedral structures with carbon atom at the center bonded to four neighboring silicon atoms. During doping incorporation, nitrogen atoms take the place of carbon atoms in tetrahedrons and bonds with the surrounding silicon atoms. The substituted nitrogen atom has a smaller radius compared with the carbon atom, which leads to a general shrinkage of the volume of the doped crystal, and thus strain is induced in the lattice. This paper reports a study of the strain induced in highly nitrogen doped 4H-SiC wafer along the growth direction and within basal plane.

## EXPERIMENT

The sample employed for this study is a chemical mechanical polished 4-inch commercial 4H-SiC wafer off-cut by 4 degrees from (0001) subjected to annealing in an elevated temperature ( $> 1000$  C). The nitrogen concentration varies across the wafer surface.<sup>3</sup> The nitrogen incorporation inside the {0001} facet region is significantly higher than the remaining area of the wafer due to the anisotropic direction dependence of nitrogen incorporation in the PVT growth process.<sup>6</sup> Using synchrotron monochromatic beam x-ray topography (SMBXT), misorientation contour map<sup>7</sup> images were recorded from the selected diffracting planes first in the  $+g$  condition and then in the  $-g$  condition by rotating  $180^\circ$  about the diffraction plane normal. The contour maps were recorded around the heavily doped facet region of the 4H-SiC wafer. We expect the doping induced strains along growth direction and the directions inside closed packed plane to be different because of the anisotropic hexagonal crystal structure of the 4H-SiC. To measure these strains, the  $g = \pm 0008$  in reflection geometry ( $c$ -axis direction only) and the  $g = \pm -2203$  in transmission geometry (both  $a$ -axis and  $c$ -axis contributions) were recorded. Because of the limitation of the incident beam size, setup geometries in reflection and transmission results in different recorded areas in wafer crystal. In reflection geometry, the entire wafer surface is illuminated while recording the  $g = \pm 0008$  diffraction at 1-BM facility in advanced photon source (APS) in Argonne National Lab. In transmission mode, only the area of beam size, which is about  $7 \times 7 \text{ mm}^2$ , is illuminated for

$g = \pm -2203$  experiments carried out at C-1 Station in Cornell High Energy Synchrotron Source (CHESS). In all our experiments, we assume that the strain measured is entirely due to impurities introduced by dopant atoms. To account for the limited beam size in transmission geometry, separate contour maps were recorded from the strained highly doped region and the unstrained unrotated reference point, by translating the wafer precisely along the rocking axis to eliminate any errors. Each contour map appears as a series of dark stripes corresponding to the series of regions that satisfy the Bragg diffraction condition as the wafer is rotated as shown as Fig. 2. Using the procedure and theory described in Ref. 6 the two sets of contour maps in  $+g$  and  $-g$  settings can be used to derive a map of strain across the heavily doped and lightly doped regions. Calculations were carried out using Wolfram's Mathematica 10.3 and Matlab R2016b software. Raman spectroscopy experiments were carried out in both heavily doped and lightly doped regions using Nomatic™ Research-Grade Raman Microscope.

## RESULTS AND DISCUSSION

### Strain Analysis Using Monochromatic Contour Mapping

In our experiments, the optical image in Fig. 1. shows the region of interest from which we recorded the  $g = \pm 0008$  contour map images. It is noticeable that the heavily doped region appears as an oval shape in a darker green contrast compared to the rest of the crystal, which is relatively lightly doped. Figure 2 shows the contour map recorded in 000-8 reflection from the same region in Fig. 1. The map

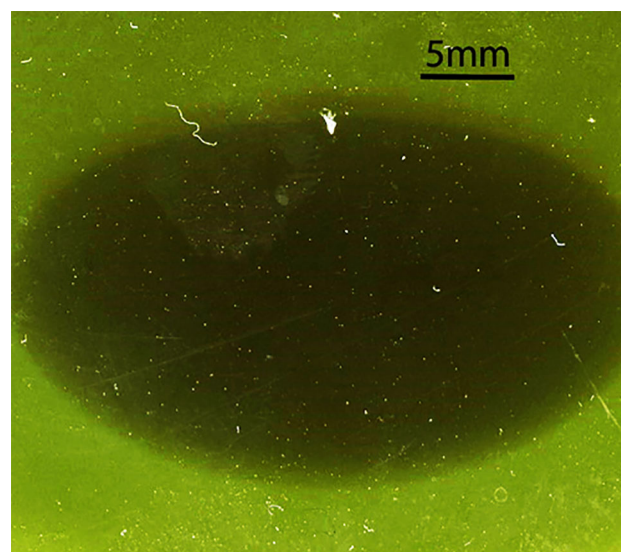


Fig. 1. Optical image of the heavily nitrogen doped region. The heavier doped region appears in a darker contrast compared to the rest of the area.

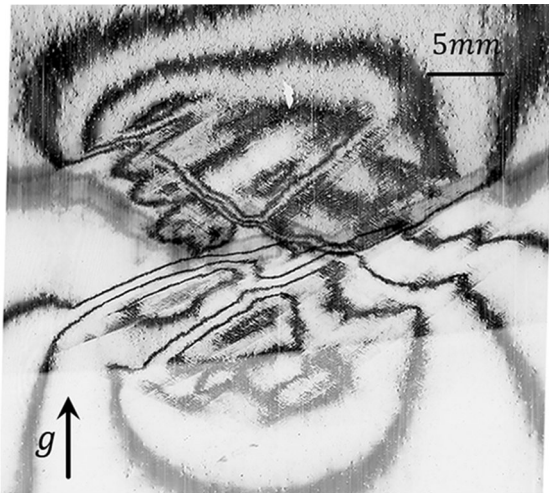


Fig. 2. Contour map recorded in  $g = 0008$ . The contours are recorded by rocking the wafer in a series of angular steps with the monochromatic X-ray beam.

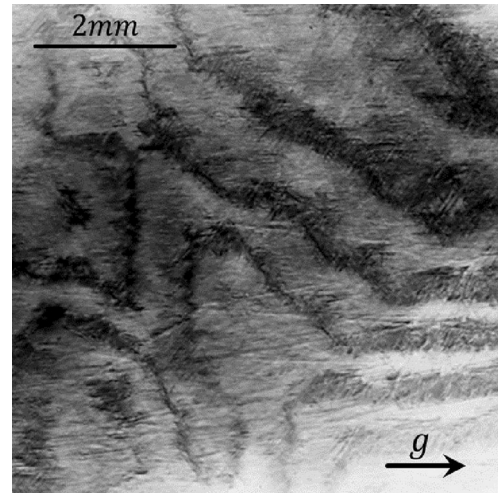


Fig. 4. Contour map recorded in  $g = 2-203$ . The contours are recorded by rocking the wafer in a series of angular steps with the monochromatic X-ray beam.

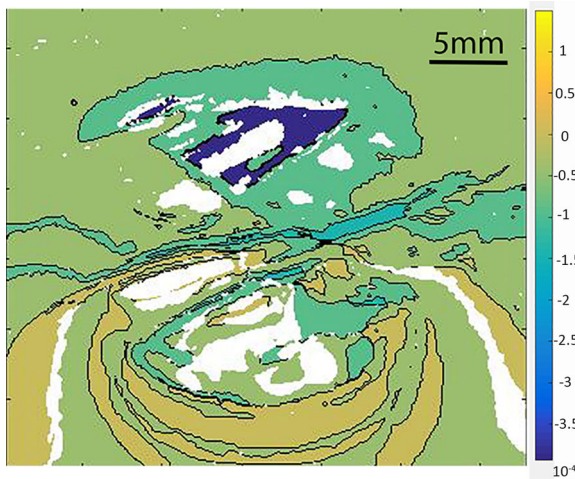


Fig. 3. Strain map simulated using the contour map by deconvoluting the lattice parameter variations from lattice tilt inside the crystal.

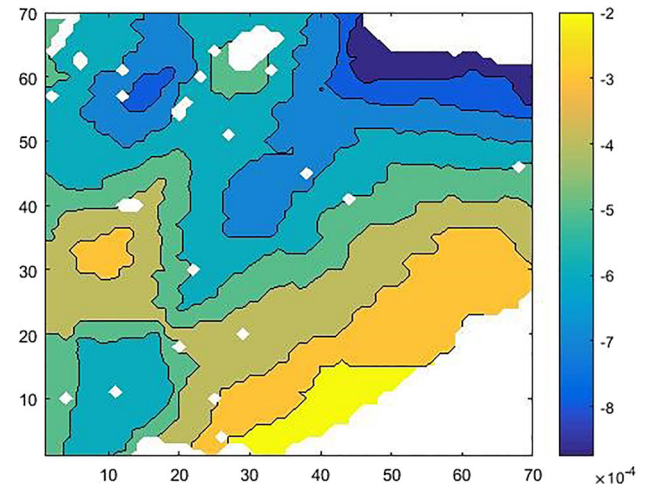


Fig. 5. Strain map simulated using the contour map by deconvoluting the lattice parameter variations from lattice tilt inside the crystal.

was recorded for the region using a  $0.003^\circ$  angular step size. Each stripe on the image represents a localized equi-inclination contour, which diffracts in the same Bragg angle condition. The narrow widths and the relatively large separation between the neighboring contours indicates local high strain. The complicated pattern, which appears like an hourglass with two concentric lobes displayed nearby the center indicates a high stress corresponding to the high doping region. The calculated strain is shown in Fig. 3. It should be noted that the white areas represent where the data were not recorded in  $g = \pm 0008$  in experiments. Figure 3 has a similar distribution as the contour map pattern, where the same color represents the average value for the corresponding region of the crystal. The negative sense of strain in general

shows an overall compression of the lattice constants along growth direction, which is in agreement with the prediction of volume shrinkage after the dopant nitrogen atoms with the smaller covalent radii substituting the intrinsic carbon atoms. The average absolute strain value inside the heavy doped oval is above  $1 \times 10^{-4}$ . The highest absolute strain is up to  $4 \times 10^{-4}$ , which appears as a deep blue color bar located inside the top lobe of the “hourglass”. This indicates the largest nitrogen incorporation level. A  $7 \times 7 \text{ mm}^2$  beam size region covering part of this most heavily doped area was selected for  $g = \pm -2203$  diffraction in transmission geometry. The contour map in  $g = 2-203$  is shown in Fig. 4, which recorded in an angular step size  $0.003^\circ$ . The corresponding strain map along this diffraction vector direction is shown in Fig. 5. The

sense of strain indicates an overall lattice compression with the magnitude ranges from  $2 \sim 8 \times 10^{-4}$ .

### Anisotropic Elasticity Model Calculating Doping Level from Strain

The 4H-SiC single crystal has a hexagonal crystal structure, which is highly anisotropic with the elastic properties different in basal plane and  $c$ -axis. According to Fig. 3, the strain inside the high doping region is very large, while outside the high doping region is negligible. It is reasonable to assume that the strain in our crystal is mainly introduced by doping. Assuming the doping atoms are locally uniformly distributed, the whole bulk crystal could be modeled as a number of rectangular prism units with the two square faces on basal planes and the longer edge aligned along [0001] direction. Each isolated rectangular prism unit is occupied by one dopant atom, as shown in the schematic (Fig. 6). The edge lengths of the square faces and the height are  $A$  and  $C$ , which equals the average distance between dopant atoms within the basal plane and along the [0001] direction, respectively. In order to represent better the rectangular prism model, the orthogonal coordinate is transformed from HCP crystal structure, where  $x = [2\bar{1}10]$ ,  $y = [01\bar{1}0]$ ,  $z = [0001]$ .

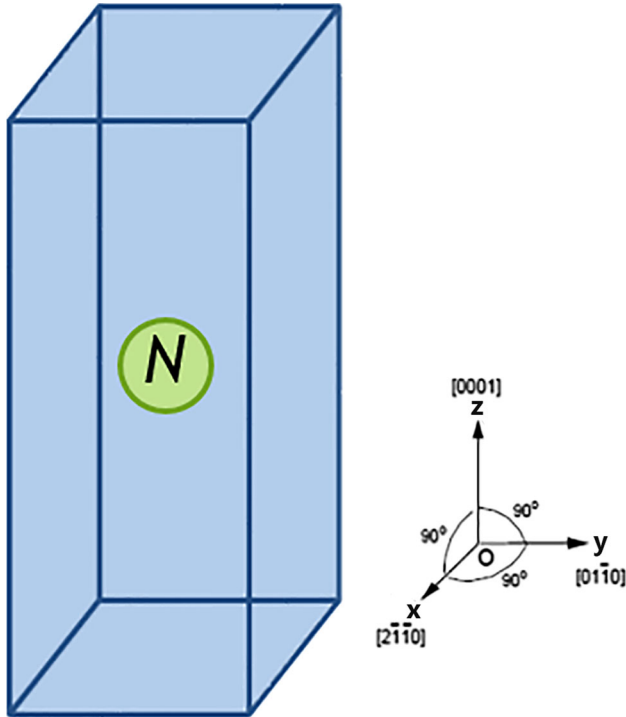


Fig. 6. The entire bulk 4H-SiC crystal was considered as a collection of rectangular prism units with one nitrogen atom located in the middle. The edge lengths of the square faces and the height are  $A$  and  $C$ , which equals the average distance between dopant atoms within basal plane and along [0001] direction, respectively.

If  $N$  is the concentration (in  $\text{cm}^{-3}$ ) of the substitutional dopants, the volume  $V$  of each cubic unit can be calculated as:

$$V = \frac{1}{N} = A^2 \times C;$$

Thus,  $C$  can be written as

$$C = \frac{1}{N \times A^2} \quad (1)$$

The origin of the change in volume after incorporating a dopant atom is due to the intrinsic size difference, which can be calculated as<sup>8</sup>:

$$\Delta v_i = \frac{4\pi}{3} [r_N^3 - r_C^3] = -0.385 \times 10^{-30} \text{ m}^3; \quad (2)$$

where  $r_C$ , and  $r_N$  are the tetrahedral covalent radii of  $C$  and  $N$  dopant,<sup>9</sup> respectively.

This amount of volume change can also lead to a three-dimensional dilation or shrinkage of the bulk crystal, which can be expressed by the displacements of an individual rectangular prism unit. According to continuum elasticity theory,

$$\Delta v_i = [V + u(\Delta v)] - V = [A + u(A)]^2 \times [C + u(C)] - A^2 \times C; \quad (3)$$

where  $u(A)$  and  $u(C)$  are the displacements along each edge of the rectangular prism after incorporating a nitrogen.

Here, the displacements  $u(A)$  and  $u(C)$  can be defined by strain values in corresponding directions. We have:

$$u(A) = \varepsilon_A * A;$$

$$u(C) = \varepsilon_C * C;$$

where  $\varepsilon_A$  and  $\varepsilon_C$  are the strains along  $x$  and  $z$  directions, which can be extracted from the contour mapping results discussed above. Take the region in specimen where we measured the highest strain as an example. The strain measured in [0008] and  $[-2203]$  directions are  $-4 \times 10^{-4}$  and  $-8 \times 10^{-4}$ , respectively. In hexagonal close-packed lattice, the lattice constant in  $\langle -2203 \rangle$  directions can be calculated as  $6 \left( \frac{a^2}{3} + \frac{c^2}{4} \right)^{\frac{1}{2}}$ ,  $a$  and  $c$  are the lattice constants along  $[2\bar{1}10]$  and  $[0001]$  of perfect 4H-SiC crystal in room temperature, respectively. The strain in  $\langle -2203 \rangle$  direction can be represented by the displacement of each lattice constant,  $\Delta a$  and  $\Delta c$ .

$$\varepsilon_{[-2203]} = \frac{\sqrt{\frac{(a+\Delta a)^2}{3} + \frac{(c+\Delta c)^2}{4}}}{\sqrt{\frac{a^2}{3} + \frac{c^2}{4}}} = -8 \times 10^{-4};$$

The strain measured in [0008] equals to the strain in [0001] direction  $\varepsilon_{-C}$ , which also equals to the

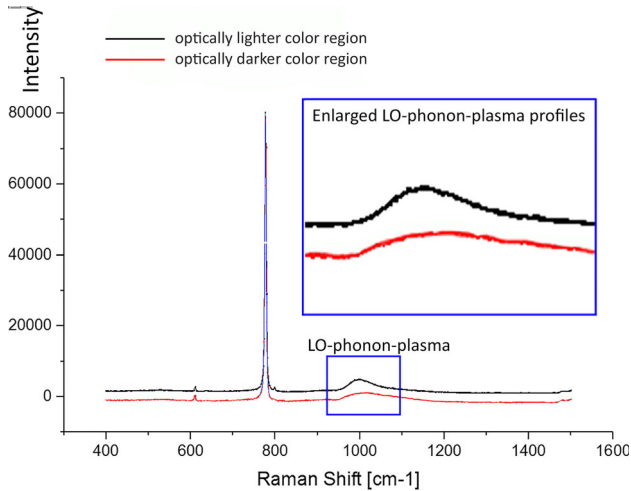


Fig. 7. Raman profiles of LO-phonon-plasmon recorded in optically lighter color region and darker color regions. As moving to the optically darker regions, the peaks of the LO-phonon-plasma are broadened and shifted to a higher frequency, which indicates a significant nitrogen concentration increase from the lighter color region to the darker color region.

value  $\Delta c/c$ . Therefore, the strain in  $[-1100]$ ,  $\varepsilon_A$  can be obtained by the expression above, which equals to  $\frac{\Delta a}{a} \sim -2.7 \times 10^{-3}$ .

Solving the simultaneous Eqs. 1, 2, and 3, we can obtain the highest doping level  $N$  inside heavily doped region of our specimen to be around  $1.5 \times 10^{20} \text{ cm}^{-3}$ . Hall Effect Measurements currently underway will be used to verify this doping concentration data.

### Correlation of Doping Concentrations with Other Measurement Techniques

Raman Spectroscopy was examined from the optically lighter green color region and the oval shape darker green color region at room temperature using a visible laser at 514 nm and spot diameter 0.104  $\mu\text{m}$ . The spectral lines of the LO-phonon-plasma in Fig. 7. shows the peaks are broadened and shift to a higher frequency as the test spots move to the optically darker region. This typical variation indicates a significant increase in the nitrogen doping level from the optically lighter to the darker regions.<sup>10</sup>

As mentioned earlier, the sample was subjected to annealing at an elevated temperature after chemical mechanical polishing. Topographic images recorded across the whole wafer using SWBXT technique showed area contrasts on  $g = 1-100$  indicating the existence of high density of double Shockley stacking faults generated inside the most heavily doped region.<sup>3</sup> Calculations done by Kuhr<sup>4</sup> indicates a threshold doping level of  $2 \times 10^{19} \text{ cm}^{-3}$  must be exceeded inside the region where the overlapping stacking faults are generated. The highest doping level in this region we calculated is

$1.5 \times 10^{20} \text{ cm}^{-3}$ , which satisfies the requirement for formation of stacking faults.

Experimental studies on lattice parameter change measurements along  $c$ -axis as a function of doping in SiC crystals reported by several other groups<sup>11,12</sup> agrees well with our results. The strain level is or the order of  $10^{-4}$  when nitrogen doping concentration is around  $1 \times 10^{20} \text{ cm}^{-3}$ . Gavrilov et al.<sup>13</sup> also reported the change is negligible in  $c$  lattice parameter compared with a lattice parameter with the increase of the nitrogen doping using the Bond method.

### CONCLUSIONS

In our study, monochromatic contour mapping technique was carried out in both reflection and transmission geometry in order to deconvolute the contribution of plane strain from the plane tilt. Anisotropic strain introduced by nitrogen incorporation in 4H-SiC bulk crystal has been analyzed via contour mapping, the highest value calculated is up to  $-4 \times 10^{-4}$  and  $-2.7 \times 10^{-3}$  along  $c$ - and  $a$ - axis respectively. The anisotropic strain originated from the different elastic properties and electric environment in closed packed plane and the growth direction inside 4H-SiC bulk crystals. The highest doping value calculated from the strain measured is up to  $1.5 \times 10^{20} \text{ cm}^{-3}$ , which exceeds the theoretical threshold doping level of around  $2 \times 10^{19} \text{ cm}^{-3}$  for spontaneously faulting at temperatures greater than  $1000^\circ\text{C}$ . The corresponding SWBXT images indicate the existence of the faulting induced by heavy doping thus verifying the doping concentration measured. The shift and broadening of LO-phonon-plasma peak in Raman Spectroscopy measurements indicates a significant increase in doping concentration of the heavy doped region inside our wafer crystal which agrees well with our measurements.

### ACKNOWLEDGEMENTS

This research used resources of the Advanced Photon Source, a U.S. Department of Energy (DOE) Office of Science User Facility operated for the DOE Office of Science by Argonne National Laboratory under Contract No. DE-AC02-06CH11357. And the Cornell High Energy Synchrotron Source (CHESS) which is supported by the National Science Foundation and the National Institutes of Health/National Institute of General Medical Sciences under NSF award DMR-1332208. Studies at APS and CHESS partly supported by Joint Photon Science Institute (JPSI).

### REFERENCES

1. T. Dalibor, G. Pensl, H. Matsunami, T. Kimoto, W.J. Choyke, A. Schöner, and N. Nordell, *Phys. Status Solidi A* 162, 199 (1997).
2. J.P. Bergman, H. Lendenmann, P.A. Nilsson, U. Lindefelt, and P. Skytt, *Mater. Sci. Forum* 353, 299 (2001).

3. Y. Yang, J. Guo, O. Goue, B. Raghoeamachar, M. Dudley, G. Chung, E. Sanchez, J. Quast, I. Manning, and D. Hansen, *J. Electron. Mater.* 45, 2066 (2016).
4. T.A. Kuhr, J. Liu, H.J. Chung, M. Skowronski, and F. Szmulowicz, *J. Appl. Phys.* 92, 5863 (2002).
5. N. Ohtani, M. Katsuno, M. Nakabayashi, T. Fujimoto, H. Tsuge, H. Yashiro, T. Aigo, H. Hirano, T. Hoshino, and K. Tatsumi, *J. Cryst. Growth* 311, 1475 (2009).
6. R.C. Glass, D. Henshall, V.F. Tsvetkov, and C.H. Carter, *MRS Bull.* 22, 30 (1997).
7. J. Guo, Y. Yang, B. Raghoeamachar, M. Dudley, and S. Stoupin, *J. Electron. Mater.* (2017). doi:[10.1007/s11664-017-5789-x](https://doi.org/10.1007/s11664-017-5789-x).
8. H. Jacobson, J. Birch, C. Hallin, A. Henry, R. Yakimova, T. Tuomi, E. Janzén, and U. Lindefelt, *Appl. Phys. Lett.* 82, 3689 (2003).
9. J.A. Van Vechten and J.C. Phillips, *Phys. Rev. B* 2, 2160 (1970).
10. H. Harima, S. Nakashima, and T. Uemura, *J. Appl. Phys.* 78, 1996 (1995).
11. R. Okojie, T. Holzheu, X. Huang, and M. Dudley, *Appl. Phys. Lett.* 83, 1971 (2003).
12. I.P. Nikitina and A.E. Nikolaev, *Diamond Relat. Mater.* 4, 784 (1995).
13. K.I. Gavrilov, V.N. Zubkov, V.G. Fomin, M.G. Shumskii, M. Shashkov, N.Y. Shushiechina, and L.A. Shegolkova, *Sov. Phys. Crystallogr.* 23, 691 (1978).